HDL-TR-2220

August 1992

Analysis of the Absorption and Emission Spectra of Mn^{5+} ($3d^2$) in $Sr_5(PO_4)_3Cl$

by John A. Capobianco
Guy Cormier
Clyde A. Morrison
Richard Moncorgé

U.S. Army Laboratory Command
Harry Diamond Laboratories
Adelphi, MD 20783-1197

Approved for public release; distribution unlimited.

The findings in this report are not to be construed as an official Department of the Army position unless so designated by other authorized documents.

Citation of manufacturer's or trade names does not constitute an official endorsement or approval of the use thereof.

Destroy this report when it is no longer needed. Do not return it to the originator.

REPORT DOCUMENTATION PAGE

Form Approved
OMB No. 0704-0188

1. AGENCY USE ONLY (Leave blank)	2. REPORT DATE	3. REPORT TYPE AND DATES COVERED
	August 1992	Final, from 8/91 to 4/92

4. TITLE AND SUBTITLE

Analysis of the Absorption and Emission Spectra of Mn^{5+} ($3d^2$) in $Sr_5(PO_4)_3Cl$

5. FUNDING NUMBERS

DA PR: AH25
PE: 6.2

6. AUTHOR(S)

John A. Capobianco and Guy Cormier, Concordia University;
Clyde A. Morrison, Harry Diamond Laboratories;
Richard Moncorgé, Université de Lyon I

7. PERFORMING ORGANIZATION NAME(S) AND ADDRESS(ES)

Harry Diamond Laboratories
2800 Powder Mill Road
Adelphi, MD 20783-1197

8. PERFORMING ORGANIZATION REPORT NUMBER

HDL-TR-2220

9. SPONSORING/MONITORING AGENCY NAME(S) AND ADDRESS(ES)

NASA Langley Research Center
Hampton, VA 23665

10. SPONSORING/MONITORING AGENCY REPORT NUMBER

11. SUPPLEMENTARY NOTES

AMS code: 612120H2500
HDL PR: 151451

12a. DISTRIBUTION/AVAILABILITY STATEMENT

Approved for public release; distribution unlimited.

12b. DISTRIBUTION CODE

13. ABSTRACT (Maximum 200 words)

The absorption and emission spectra of Mn^{5+} ($3d^2$) in $Sr_5(PO_4)_3Cl$ are analyzed using a C_4 crystal-field Hamiltonian. The descent in symmetry from cubic was guided by a point-charge calculation of the crystal-field components. The calculated energy levels are in excellent agreement with those obtained experimentally. The resulting crystal-field parameters, B_{nm}, represent very well the crystal-field interactions of Mn^{5+} in $Sr_5(PO_4)_3Cl$.

14. SUBJECT TERMS

Mn^{5+}, strontium chloroapatite, tunable lasers, absorption-emission spectra of Mn^{5+}, spectroscopy of MnO_4

15. NUMBER OF PAGES

23

16. PRICE CODE

17. SECURITY CLASSIFICATION OF REPORT	18. SECURITY CLASSIFICATION OF THIS PAGE	17. SECURITY CLASSIFICATION OF ABSTRACT	20. LIMITATION OF ABSTRACT
Unclassified	Unclassified	Unclassified	UL

Contents

Figures

Tables

1. Introduction

Currently most operating vibronic lasers are based on $3d$ ions, such as Cr^{3+}, Ti^{3+}, Co^{2+}, and Ni^{2+}. Except for Ti^{3+}, all these ions are in their common oxidation state. To increase the spectral range covered by tunable solid-state lasers, we must search for doped crystal systems based on different ions or ions in different ionization states. Recently, a new lasing ion was discovered [1], the Cr^{4+} ion. The oxidation state of chromium had not even been known to luminesce when Petricevic et al [1] and Verdún et al [2] announced that they had achieved laser action in forsterite (Mg_2SiO_4) using the Cr^{4+} ion.

Because of the novelty of Cr^{4+} as a luminescent ion and our interest in the electronic structure of higher oxidation states [3], we decided to characterize other d^2 ions in tetrahedral sites. Recently, we reported the gain measurements, emission spectra (at 77 K and room temperature), and the fluorescence lifetimes of Mn^{5+} ($3d^2$) in Ca_2PO_4Cl and $Sr_5(PO_4)_3Cl$ [4,5]. The Mn^{5+} ion is stabilized in tetraoxo coordination (MnO_4^{3-}) by isomorphous substitution of the PO_4^{3-} ion.

Crystal-field theory predicts that the energy-level sequence for a d^2 ion in a tetrahedral environment should be $^3A_2 < {}^1E < {}^1A_1 < {}^3T_2 < {}^3T_1(P) < {}^1T_2 < {}^1T_1 < {}^3T_1(F)$. The order is the one that would be expected from the Tanabe-Sugano diagram with $Dq/B \approx 3$. The only allowed transition (electric dipole) is the $^3T_1 \leftarrow {}^3A_2$ in an undisturbed T_D symmetry. However, it follows that most of the features of the spectra observed by us [4,5] and other workers [6–10] must be interpreted as resulting from a distortion of the MnO_4^{3-} from T_D symmetry.

In the present work, we undertake a systematic analysis of the optical spectra (absorption and emission) of the Mn^{5+} ion in $Sr_5(PO_4)_3Cl$, by using a crystal-field Hamiltonian of C_4 point symmetry. In the analysis, the energy-level scheme for Mn^{5+}-doped $Sr_5(PO_4)_3Cl$ is determined, and the crystal-field parameters are obtained.

2. Experiment

Single crystals of MnO_4^{3-} doped $Sr_5(PO_4)_3Cl$ were grown from flux with a procedure modified from that of Borromei and Fiscaro [8,9]. The concentration of manganese in the $Sr_5(PO_4)_3Cl$ crystal was found to be 0.033 wt% (4.145×10^{18} ions/cm^3).

Emission spectra at 77 K and room temperature were made with the 514.5-nm green line of a Coherent CR-18 argon ion laser. The spectra were recorded with a Jarrell-Ash 3/4m monochromator in second order. The fluorescence signal was monitored with a Northcoast (model EO-817P) liquid-nitrogen-cooled germanium detector and analyzed with a Stanford SR510 lock-in amplifier. The absorption spectrum was obtained with a Varian Cary 2400 spectrophotometer. The observed absorption and emission peaks are presented in section 5. The emission spectra are shown in figure 1.

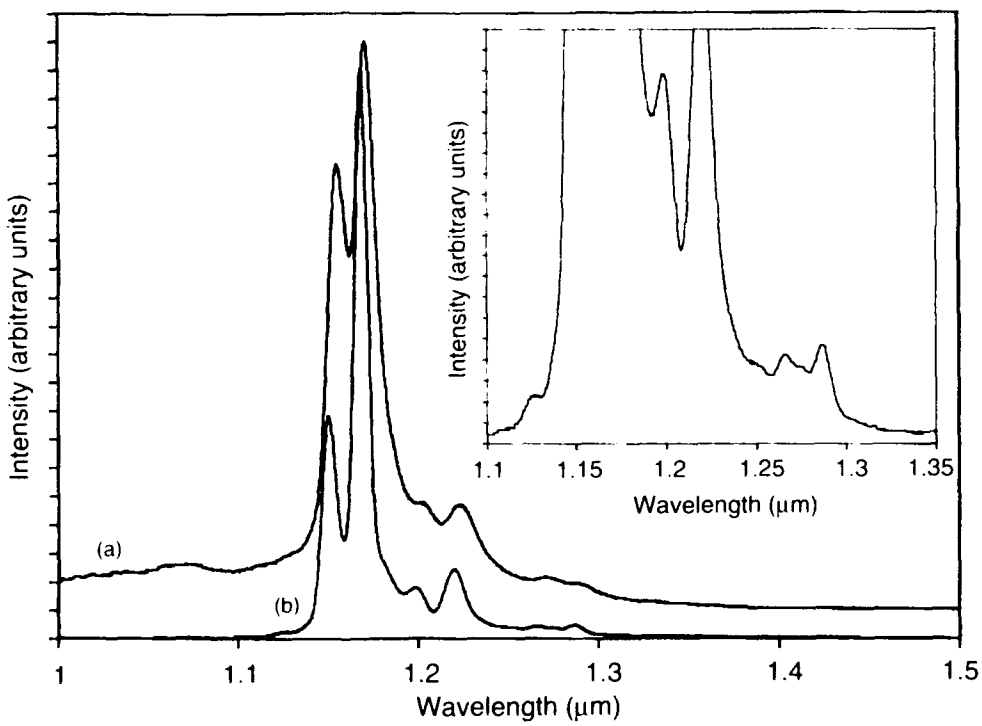

Figure 1. Emission spectrum of $Sr_5(PO_4)_3Cl:MnO_4^{3-}$: (a) 300 K, (b) 77 K excited at 514.5 nm. Inset shows vibrational details at 77 K.

3. Free-Ion Hamiltonian

The free-ion Hamiltonian, H_{FI}, used in the analysis of the spectrum of Mn^{5+} ($3d^2$) is

$$H_{FI} = F^{(2)}g_2 + F^{(4)}g_4 + \alpha L(L+1) + \zeta_d \sum_i \dot{l}_i \cdot \dot{s}_i \ . \tag{1}$$

where

$$g_k = \sum_{i>j} \sum_{q=-k}^{k} C^{*}_{kq}(i)\, C_{kq}(j) \ . \tag{2}$$

and

$$C_{kq}(i) = \sqrt{4\pi/(2k+1)}\ Y_{kq}(\theta_i, \varphi_i) \ . \tag{3}$$

$$C^{*}_{kq} = (-1)^q C_{k-q} \ .$$

In equation (1), ζ_d is the spin-orbit parameter, the term involving α is the Trees interaction [11], and the $F^{(k)}$ are the Slater parameters. Frequently, the Racah parameters B and C are used in place of the Slater parameters $F^{(k)}$: the relations

$$F^{(2)} = 7(7B + C) \quad \text{and}$$

$$F^{(4)} = 63C/5 \tag{4}$$

can be used to convert from one set of parameters to the other. The different sets of values of $F^{(k)}$, B, and C are given in table 1, calculated using Hartree-Fock wavefunctions [12] and best fit, using equation (1), to the free-ion experimental energy levels of Corliss and Sugar [13]. The fourth column gives the values obtained by Kingsley et al [10] by fitting the experimental data on Mn^{5+} in $Ca_5(PO_4)_3Cl$ (with $\alpha = 0$), which is isomorphic to the material under consideration. In general, the Hartree-Fock values of the Slater parameters are larger than the free-ion values, and these parameters are further reduced when the ion is embedded in a solid. In other words, the sequence of reduction of the $F^{(k)}$ in going from columns 2 through 4 is typical of both rare-earth and transition-metal ions. A theory of the reduction of the Slater parameters, $F^{(k)}$, upon the ion entering a solid has been given by Morrison [14] (pp 74,75), which is

$$F^{(k)} = F^{(k)}_{0} - \Delta F^{(k)}$$

with

$$\Delta F^{(k)} = \langle r^k \rangle^2 S^{(k)} \ , \tag{5}$$

where the $\langle r^k \rangle$ are the radial expectation values of r^k, $F_0^{(k)}$ are the free-ion Slater parameters, and $S^{(k)}$ is a sum over the ligands of the solid, given in section 4.

Table 1. Values of free-ion parameters of Mn^{5+}

Parameter	Hartree-Fock[a]	Free ion[b]	$Ca_5(PO_4)_3Cl$[c]	$Sr_5(PO_4)_3Cl$[d]
$F^{(2)}$	108.746	91.427	42.735	39.925
$F^{(4)}$	68.880	56.625	28.413	33.861
B	1.434	1.224	550	431
C	5.467	4.494	2.255	2.687
ζ	486.0	465.8	0	0
α	--	106.4	0	39

[a] *Fraga et al [12].*
[b] *Fit to data of Corliss and Sugar [13].*
[c] *Kingsley et al [10].*
[d] *Best fit to cubic obtained here.*

4. Crystallographic Data and Crystal-Field Components

The detailed crystallographic analysis of $Sr_5(PO_4)_3Cl$ has been performed by Sudarsanan and Young [15] and the results are given in table 2, along with data on polarizabilities from Schmidt et al [16].

The polarizabilities, α, and the detailed x-ray data given in table 2 have been used to calculate the sums, $S^{(k)}$, to be used in equation (5). That is, we evaluate

$$S^{(k)} = e^2 \sum_i \frac{\alpha_i Z_i (k+1)}{R_i^{2k+4}} \quad , \tag{6}$$

where α_i is the ligand polarizability (given in table 2) with the number of ligands, Z_i, at the distance R_i from the P ion site. The values obtained are $S^{(2)} = 59.825\ cm^{-1}/Å^4$ and $S^{(4)} = 17.661\ cm^{-1}/Å^8$.

The point-charge crystal-field [9] components, A_{nm}, were computed using

$$A_{nm} = -e^2 \sum_i q_i \frac{C_{nm}(\hat{R}_i)}{R_i^{n+1}} \quad , \tag{7}$$

where q_i is the charge (in units of electron charge) given in table 2 and the C_{nm} are defined in equation (3). These results are given in table 3.

Table 2. Crystallographic data [15] on $Sr_5(PO_4)_3Cl$: Hexagonal C_{6h}^2 ($P6_3/m$), 176, $Z = 2$

Ion	Site	Symmetry	x	y	z	q	α (Å^3)[a]
O1	6*h*	C_s	0.3365	0.4821	1/4	−2	1.349
O2	6*h*	C_s	0.5861	0.4662	1/4	−2	1.349
O3	12*i*	C_1	0.3549	0.2670	0.0768	−2	1.349
P	6*h*	C_s	0.4052	0.3720	1/4	5	0.0273
Sr1	4*f*	C_3	1/3	2/3	0.0009	2	1.039
Sr2	6*h*	C_s	0.0104	0.2592	1/4	2	1.039
Cl	2*b*	C_{3i}	0	0	1/2	−1	2.694

[a] *Schmidt et al [16].*

Note: x ray data: a = 9.859 and c = 7.206 A [16].

Distance (A) of nearest neighbors to P site: two O3 ions at 1.5368, one O1 ion at 1.5402, one O2 ion at 1.5450 A. Smallest P to P distance is 4.2577 A (double).

Table 3. Monopole (point-charge) crystal-field components, A_{nm} (cm^{-1}/A^n), for P site (C_s symmetry) in $Sr_5(PO_4)_3Cl$[a]

A_{nm}	ReA_{nm}	ImA_{nm}	A_{nm}	ReA_{nm}	ImA_{nm}
A_{11}	111.6	3.084	A_{42}	−16.869	29.618
A_{20}	1.183	—	A_{44}	12.647	12.900
A_{22}	−4.477	−2.956	A_{51}	−740.1	−55.74
A_{31}	34.779	58.472	A_{53}	618.9	−3.101
A_{33}	52.251	6.065	A_{55}	−53.07	1.381
A_{40}	9.151	—			

[a] *X-ray data from table 3.*

In the calculations involving the crystal fields, it is assumed that the A_{nm} with even n contribute to the crystal-field splitting, while the A_{nm} with odd n contribute to the electric dipole transition probabilities. Owing to the rather large values of the A_{nm} with n odd, we should expect the electric dipole transitions to be strong for those levels where the transition is not spin forbidden [17–19].

The crystal-field components of table 3 are correct for the P site, which has C_s symmetry and bears little resemblance to tetrahedral cubic symmetry ($A_{2m} = 0$, $A_{4m} = 0$, except A_{40} and A_{44} in cubic symmetry). To see the resemblance to cubic symmetry, we rotate the A_{nm} through the Euler angles (α, β, and γ) by using [20]

$$A'_{nm} = \sum_{m'} D^{n}_{m'm}(\alpha,\beta,\gamma)A_{nm'}. \tag{8}$$

By evaluating the A'_{nm} with even n for a variety of values of α, β, and γ, and by using the A_{nm} of table 2, we obtained (units of A'_{nm} are $\mathrm{cm}^{-1}/\mathrm{\AA}^n$)

$$\begin{aligned}
A'_{20} &= 493, \\
A'_{21} &= -494 - i380, \\
A'_{22} &= 801 - i3750, \\
A'_{40} &= -41{,}974, \\
A'_{41} &= 613 + i1631, \\
A'_{42} &= -1.7 + i2002, \\
A'_{43} &= 1512 + i2876, \\
A'_{44} &= -25{,}129 - i146,
\end{aligned} \tag{9}$$

with $\alpha = 30°$, $\beta = 45°$, and $\gamma = 1.5°$.

Further choices of α, β, and γ might reduce A'_{41}, A'_{42}, and A'_{43}, but these values are adequate for our purposes. For perfect cubic symmetry, A'_{2m} should be zero, and $A'_{41} = A'_{43} = 0$ with $A'_{44} = \sqrt{5/14}\, A'_{40}$. From equation (9), we have $A_{44} \approx 0.5987 A'_{40}$ ($\sqrt{5/14} \approx 0.5976$), so that if we ignore A'_{41}, A'_{42}, and A'_{43} relative to A'_{40}, we have cubic symmetry. Further, since $A'_{40} < 0$, we have tetrahedral symmetry. The A'_{2m} which is ignored in the cubic approximation will contribute to the splitting of the cubic levels.

5. Analysis of Experimental Data

The crystal-field Hamiltonian, H_{CEF}, for the configuration d^2, which we use in the analysis, can generally be written

$$H_{CEF} = \sum_{n \text{ even}} \sum_{m=-n}^{n} B^{*}_{nm} \sum_{i} C_{nm}(i) \quad , \tag{10}$$

$$B^{*}_{nm} = (-1)^{m} B_{n-m} \quad ,$$

where the B_{nm} are the crystal-field parameters. The B_{nm} of equation (10) are treated as parameters in fitting the energy levels of the ion in a crystal, in the same manner as the $F^{(k)}$ are treated as parameters in fitting the free-ion data. In the point-ion model, these parameters are related to the A_{nm} by

$$B_{nm} = \langle r^{n} \rangle A_{nm} \quad . \tag{11}$$

For the ion in C_s symmetry (from equation (11) and table 3) (see Morrison [14], pp 86, 87), we have eight B_{nm} (n even) which can be reduced to seven by a simple rotation about the z-axis (c-axis). With the free-ion parameters $F^{(k)}$ and α, we have a total of 10 parameters. This large number of parameters requires an extensive number of energy levels, generally beyond the number of levels available. Because of the limited number of crystal-field levels experimentally available, we decided to use C_4 symmetry in the final analysis of the data. In C_4 symmetry, equation (10) becomes

$$H^{(4)}_{CEF} = B_{20} \sum_{i} C_{20}(i) + B_{40} \sum_{i} C_{40}(i) + B_{44} \sum_{i} C_{44}(i) + C_{4-4}(i) \tag{12}$$

with all B_{nm} real. The cubic approximation to equation (12) is

$$H^{(4)}_{CEF} = B^{c}_{40} \sum_{i} \left\{ C_{40}(i) + \sqrt{\frac{5}{14}} \, C_{44}(i) + C_{4-4}(i) \right\} \tag{13}$$

with $B^{c}_{40} = -21|Dq|$, for tetrahedral symmetry.

We start the fitting of the experimental data by using the cubic approximation given in equation (13). Using the results of the cubic fitting, we then proceed to fit the data in C_4 symmetry using equation (12). In both of these analyses, we ignore the effects created by the spin-orbit coupling of equation (1). Finally, we introduce all the experimental data with the spin-orbit coupling included.

The absorption spectra taken at low temperature show two intense bands at 10,600 and 11,250 cm^{-1}; from a Tanabe-Sugano plot for tetrahedral symmetry (fig. 2), we find that a rough estimate of absorption spectra fits the plot with $Dq/B \approx 2.0$ (assuming that $10Dq \approx 11{,}000$). Then we have $B_{40} \approx -23{,}100\ cm^{-1}$ ($B_{44} = \sqrt{5/14}\ B_{40}$) and $B = 550\ cm^{-1}$; with $C/B \approx 4$ we have $C = 2200\ cm^{-1}$. Thus we have $F^{(2)} = 42{,}350$, $F^{(4)} = 27{,}720$, and $B_{40} = -23{,}100\ cm^{-1}$ as starting values in equation (1) ($\zeta = 0$) and equation (13) for the first fitting of the experimental data. In the initial phase of the fitting, the parameter α was arbitrarily set at 30 cm^{-1} and not varied. The best fit to the

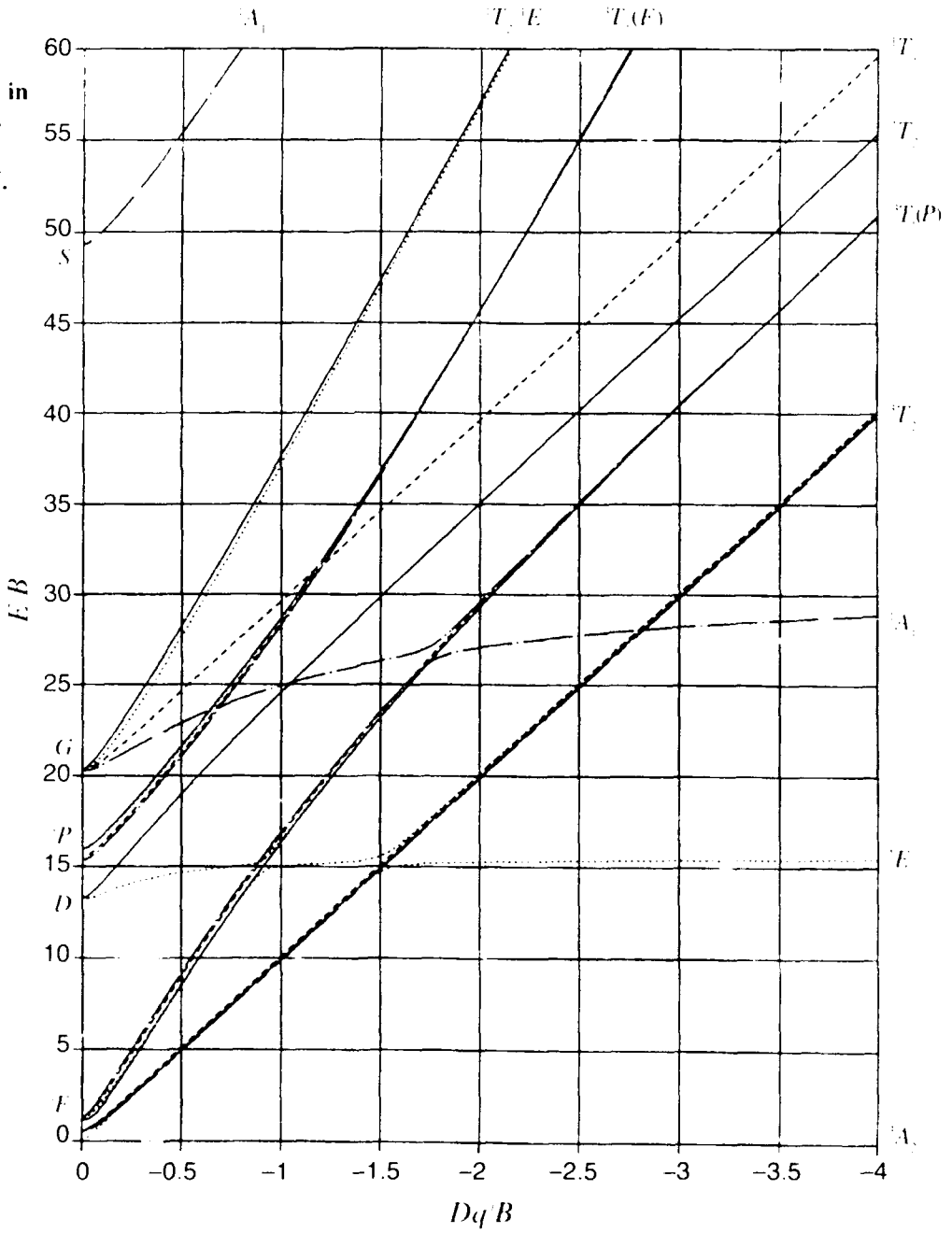

Figure 2. Tanabe-Sugano plot for Mn^{5+} in tetrahedral symmetry using Hartree-Fock values for B, C, and ζ.

Mn^{5+} (d^2) $Dq/B < 0$
solid line — gamma 5
dashed — gamma 4
dotted — gamma 3
chain dash — gamma 2
chain dot — gamma 1
$C/B = 3.801$
$\zeta/B = 0.338$

experimental data (averaged to cubic symmetry), starting with the above parameters, is given in table 4. The last column in table 5 gives the mixture of free-ion states; we see that since there is only one $^3A_2$, $^3T_2$, and $^1T_1$ in the decomposition of the $3d^2$ electron configuration on the cubic group (no spin orbit), these states remain pure, as they should. However, the $^3T_1$ states become strongly mixed, the $^3T_1$ at 15,400 cm^{-1} is 54-percent ^3P and 46-percent ^3F, while the $^3T_1$ at 24,200 cm^{-1} has the reversed composition of free-ion states. This strong mixture is a consequence of both the reduced $F^{(k)}$ values and the relatively strong crystal field. Even the $^1A_1$ at 45,760 cm^{-1}, which is normally 100-percent ^1S, has 15-percent ^1G free-ion state.

In order to proceed to the analysis of the energy levels in the assumed C_4 symmetry, we need an estimate of the parameter B_{20}. We can estimate B_{20} by using equation (5) with the $F_0^{(2)}$ value from table 2 (free-ion $F^{(2)}$) and $F^{(2)}$ from table 4 to obtain $\langle r^2 \rangle = 0.93$ Å^2. This value is then used with A'_{20} from equation (9) to give $B_{20} \approx 457$ cm^{-1}. With all the parameters the same as the cubic case, the experimental data on the ^1E and the $^3T_2$ were changed, and the parameters were varied to obtain a best fit. The results are given in table 5. The calculated splitting of the ^1E cubic level by the lower symmetry is considerably less than the experimental value, but the calculated splitting of the $^3T_2$ level is quite close to the observed value. If all the experimental data are removed (including the ground state) except the ^1E levels (8550 and 8697 cm^{-1}), and if we then vary B_{20} (with all other parameters fixed at the values given in table 6), these levels are fit exactly with $B_{20} = 2607$ cm^{-1}. If the ground state is included ($\Gamma_{3,4}E = 0$) as well as the ^1E levels, varying $F^{(2)}$ and B_{20} produces an exact fit with $F^{(2)} = 42{,}456$ and $B_{20} = 2640$ cm^{-1}. In both these fitting procedures, the free-ion admixture of the ^1E state remained the

Table 4. Mn^{5+} energy levels in $Sr_5(PO_4)_3Cl$, tetrahedral symmetry, no spin orbit[a]

No.	I.R.[b]	E_{exp} (cm^{-1})	E_{theo} (cm^{-1})	Free-ion state[c]
1	$^3A_2$	0	−257	1.00 ^3F
2	^1E	8,619	8,433	0.64 ^1D + 0.36 ^1G
3	$^3T_2$	11,000	11,095	1.00 ^3F
4	$^1A_1$	14,960	14,963	0.85 ^1G + 0.15 ^1S
5	$^3T_1(P)$	15,400	15,256	0.54 ^3P + 0.46 ^3F
6	$^1T_2$	19,600	19,662	0.71 ^1D + 0.29 ^1G
7	$^1T_1$	21,560	21,949	1.00 ^1G
8	$^3T_1(F)$	24,200	24,368	0.54 ^3F + 0.46 ^3P
9	^1E	31,343	31,910	0.64 ^1G + 0.36 ^1D
10	$^1T_2$	33,110	32,033	0.71 ^1G + 0.29 ^1D
11	$^1A_1$	45,760	45,913	0.85 ^1S + 0.15 ^1G

[a]Parameters (cm^{-1}) used in this calculation are $F^{(2)} = 39{,}925$, $F^{(4)} = 33{,}861$, $\alpha = 38.62$, $B_{40} = -23{,}840$, $B_{44} = -14{,}247.12$ ($B = 430.88$, $C = 2687.4$, $Dq = 1100$).

[b]Irreducible representation of O group.

[c]Only levels with mixture >0.01 are listed, and number is limited to 3.

same as that given in table 6; however, the splittings of the higher levels become significantly different from the experimental results given in table 6. Also, in table 4 the lowest $^3T_1$ splitting remains $^3T_1(P)$ and is close to the observed value, but the highest energy splitting has become predominantly ^3F. The same is true of the higher $^3T_1(F)$ level, except that the lowest values have become predominantly ^3P.

Finally, starting with the same parameters as were used in table 5, we fitted the same experimental data except that the spin-orbit interaction was included with $\zeta = 466\ \text{cm}^{-1}$ (free-ion value). After a few trials varying ζ to obtain a best fit, we decided to leave ζ at the free-ion value, as it seems that more experimental splittings are necessary to stabilize the best-fit value of ζ. The results of this calculation are given in table 6. (The labeling of the levels follows the convention introduced by Ballhausen and Liehr [21]. That is, when the spin-orbit interaction is included in the calculation, the irreducible representation labels are the Γ_i from Bethe; otherwise, the A, B, and E from Mulliken are used.)

Table 5. Mn^{5+} energy levels in $Sr_5(PO_4)_3Cl$, C_4 symmetry, no spin orbit[a]

No.	I.R.[b]	E_{exp} (cm^{-1})	E_{theo} (cm^{-1})	Free-ion composition[c]
1	$^3A_2$	0	−118	1.00 ^3F
2	$^1A_1$	8,550[d]	8,543	0.65 ^1D + 0.34 ^1G
3	$^1A_2$	8,687[d]	8,624	0.66 ^1D + 0.34 ^1G
4	$^3A_2$	10,600	10,699	1.00 ^3F
5	^3E	11,250	11,319	1.00 ^3F
6	$^3A_1$	14,750	14,653	0.55 ^3P + 0.45 ^3F
7	$^1A_1$	14,960	15,529	0.84 ^1G + 0.15 ^1S + 0.01 ^1D
8	^3E	16,275	16,136	0.54 ^3F + 0.46 ^3P
9	$^1A_2$	19,600	19,295	0.72 ^1D + 0.28 ^1G
10	^1E	—	19,853	0.73 ^1D + 0.27 ^1G
11	$^1A_1$	21,560	21,320	1.00 ^1G
12	^1E	—	23,090	0.99 ^1G + 0.01 ^1D
13	^3E	24,200	24,357	0.54 ^3P + 0.46 ^3F
14	$^3A_1$	—	25,270	0.55 ^3F + 0.45 ^3P
15	$^1A_1$	31,343	31,238	0.66 ^1G + 0.33 ^1D + 0.01 ^1S
16	^1E	—	31,887	0.74 ^1G + 0.26 ^1D
17	$^1A_2$	33,110	32,879	0.66 ^1G + 0.34 ^1D
18	$^1A_2$	—	33,025	0.72 ^1G + 0.28 ^1D
19	$^1A_1$	45,760	45,812	0.84 ^1S + 0.16 ^1G

[a] *Parameters (cm^{-1}) used in this calculation are $F^{(2)} = 41{,}565$, $F^{(4)} = 31{,}460$, $\alpha = 57.76$, $B_{20} = 1923$, $B_{40} = -24{,}251$, and $B_{44} = -13{,}576$ ($B = 491.58$ and $C = 2497$).*

[b] *Irreducible representations of C_4 group.*

[c] *Only levels with mixture >0.01 are listed, and number is limited to 3.*

[d] *Obtained from emission spectrum.*

Table 6. Mn^{5+} energy levels in $Sr_5(PO_4)_3Cl$, C_4 symmetry with spin orbit included[a]

No.	I.R.[b]	E_{exp} (cm^{-1})	E_{theo} (cm^{-1})	Free ion composition[c]
1	$\Gamma_{3,4}$	0	−74	1.00 ^3F
2	Γ_2	—	−73	1.00 ^3F
3	Γ_1	8,550	8,456	0.63 ^1D + 0.32 ^1G + 0.04 ^3F
4	Γ_2	8,687	8,502	0.62 ^1D + 0.31 ^1G + 0.07 ^3F
5	$\Gamma_{3,4}$	10,600	10,685	1.00 ^3F
6	Γ_2	—	10,714	0.97 ^3F + 0.02 ^1D + 0.01 ^1G
7	Γ_2	—	11,207	0.99 ^3F
8	Γ_2	—	11,302	0.96 ^3F + 0.03 ^1D + 0.01 ^1G
9	$\Gamma_{3,4}$	11,250	11,351	0.99 ^3F
10	Γ_1	—	11,481	1.00 ^3F
11	Γ_1	—	11,544	0.95 ^3F + 0.03 ^1D + 0.01 ^1G
12	Γ_1	14,750	14,622	0.50 ^3P + 0.40 ^3F + 0.08 ^1G
13	$\Gamma_{3,4}$	—	14,673	0.55 ^3P + 0.45 ^3F
14	Γ_1	14,960	15,403	0.49 ^1G + 0.22 ^3F + 0.20 ^3P
15	Γ_2	16,275	16,088	0.57 ^3F + 0.43 ^3P
16	$\Gamma_{3,4}$	—	16,127	0.53 ^3F + 0.46 ^3P
17	Γ_2	—	16,146	0.57 ^3F + 0.42 ^3P + 0.01 ^1G
18	Γ_1	—	16,161	0.50 ^3F + 0.50 ^3P
19	Γ_1	—	16,534	0.35 ^3P + 0.33 ^3F + 0.28 ^1G
20	Γ_2	—	19,218	0.71 ^1D + 0.27 ^1G + 0.01 ^3F
21	$\Gamma_{3,4}$	19,600	19,802	0.73 ^1D + 0.25 ^1G + 0.01 ^3F
22	Γ_1	21,560	21,502	0.99 ^1G + 0.01 ^3P
23	$\Gamma_{3,4}$	—	23,209	0.96 ^1G + 0.02 ^3P + 0.01 ^3F
24	Γ_2	24,200	24,295	0.57 ^3P + 0.43 ^3F
25	Γ_1	—	24,351	0.51 ^3P + 0.49 ^3F
26	Γ_2	—	24,363	0.56 ^3P + 0.42 ^3F + 0.01 ^1G
27	$\Gamma_{3,4}$	—	24,387	0.52 ^3P + 0.45 ^3F + 0.02 ^1G
28	Γ_1	—	24,390	0.50 ^3F + 0.49 ^3P + 0.01 ^1G
29	Γ_1	—	25,254	0.56 ^3F + 0.44 ^3P
30	$\Gamma_{3,4}$	—	25,307	0.55 ^3F + 0.43 ^3P + 0.02 ^1G
31	Γ_1	31,343	31,309	0.66 ^1G + 0.33 ^1D + 0.01 ^1S
32	$\Gamma_{3,4}$	—	31,972	0.74 ^1G + 0.25 ^1D
33	Γ_2	33,110	32,946	0.66 ^1G + 0.34 ^1D
34	Γ_2	—	33,104	0.72 ^1G + 0.28 ^1D
35	Γ_1	45,760	45,751	0.83 ^1S + 0.16 ^1G

[a]Parameters (cm^{-1}) used in this calculation are $F^{(2)} = 41,677$, $F^{(4)} = 31,341$, $\alpha = 71$, $\zeta = 466$ (not varied), $B_{20} = 1881$, $B_{40} = -24,161$, and $B_{44} = -13,480$ ($B = 495.23$, $C = 2487.4$).

[b]Irreducible representations of C_4 group (Bethe notation). $\Gamma_3 + \Gamma_4 = \Gamma_{3,4}$.

[c]Only levels with mixtures >0.01 are listed, and number is limited to 3.

The most important result of the spin-orbit interaction is the mixing of the different spin states. For example, the ^1E state in cubic symmetry which becomes the $^1A_1$, $^1A_2$, in C_4 symmetry contains 4- to 7-percent ^3F, and the $^1A_1$ (cubic) becomes 22-percent ^3F and 20-percent ^3P. This mixing of triplet states into what are normally labeled *singlets* has the effect of allowing transitions such as the ^1A to be observed. The ground state splitting of 0.8 cm^{-1} is in reasonable agreement with the value observed by Lachwa and Reinen [22] using an electron spin resonance technique. The resulting parameters in the various fittings reported above are summarized in table 7. However, since the ground state is the doublet $\Gamma_3 + \Gamma_4$ in C_4 symmetry, which splits further under a crystal field of C_s symmetry, this agreement should be viewed with skepticism.

Table 7. Parameters (cm^{-1}) that best fit experimental data for Mn^{5+} in $Sr_5(PO_4)_3Cl$

Symmetry	$F^{(2)}$	$F^{(4)}$	α	ζ	B_{20}	B_{40}	B_{44}	Table No.
Cubic	39,925	33,861	38.6	0	0	−23,840	−14,247.1	4
C_4	41,565	31,460	57.8	0	1923	−24,251	−13,576	5
C_4	41,677	31,341	71	466	1881	−24,161	−13,480	6

6. Conclusions

The computational procedure used here gives excellent agreement between the experimental and calculated energy levels. Thus, we feel that the resulting crystal-field parameters given in table 6 are a valid representation of the crystal-field interactions of Mn^{5+} in $Sr_5(PO_4)_3Cl$. The results indicate the adequacy of using a crystal-field Hamiltonian of C_4 symmetry.

Acknowledgements

The authors gratefully acknowledge the Natural Science and Engineering Council of Canada, and the Centre National de la Récherche Scientifique of France for financial support. Also, CAM appreciates the helpful discussions with his associates, John D. Bruno and Richard P. Leavitt.

References

1. V. Petricevic, S. K. Gayen, and R. R. Alfano, in *OSA Proceedings on Tunable Solid State Lasers*, edited by M. L. Shand and H. P. Jenssen, Optical Society of America, Washington, DC (1989), p 77.

2. H. R. Verdún, L. M. Thomas, D. M. Andrauskas, and A. Pinto, in *OSA Proceedings on Tunable Solid State Lasers*, edited by M. L. Shand and H. P. Jenssen, Optical Society of America, Washington, DC (1989), p 85.

3. R. Moncorgé, D. J. Simkin, G. Cormier, and J. A. Capobianco, in *OSA Proceedings on Tunable Solid State Lasers*, edited by M. L. Shand and H. P. Jenssen, Optical Society of America, Washington, DC (1989), p 93.

4. J. A. Capobianco, G. Cormier, H. Manaa, R. Moncorgé, M. Bettinelli, P. Galarneau, and B. Labranche, *Proceedings of Advanced Solid State Lasers*, Hilton Head, SC (18–20 March 1991).

5. J. A. Capobianco, G. Cormier, R. Moncorgé, H. Manaa, and M. Bettinelli, Appl. Phys. Lett. **60** (1991), 163.

6. C. Simo, E. Banks, and S. L. Holt, Inorg. Chem. **9** (1970), 183.

7. J. B. Milstein, J. Ackerman, S. L. Holt, and B. R. McGarvey, Inorg. Chem. **11** (1972), 1178.

8. R. Borromei, L. Oleari, and P. Day, J. Chem. Soc. Faraday Trans. 2 **77** (1981), 1563.

9. R. Borromei and E. Fisicaro, Gazz. Chim. Ital. **109** (1979), 191.

10. J. D. Kingsley, J. S. Prener, and B. Segall, Phys. Rev. **137** (1965), A189.

11. R. E. Trees, J. Opt. Soc. Am. **54** (1964), 651.

12. S. Fraga, K.M.S. Saxena, and J. Karwowski, in *Handbook of Atomic Data*, Physical Science Data **5**, Elsevier, New York (1976).

13. C. Corliss and J. Sugar, J. Phys. Chem. Ref. Data **6** (1965), 1253.

14. C. A. Morrison, *Angular Momentum Theory Applied to Interactions in Solids*, Lecture Notes in Chemistry **47**, Springer-Verlag, New York (1988).

15. K. Sudarsanan and R. A. Young, Acta Crystallogr. **B30** (1974), 1381.

16. P. C. Schmidt, A. Weiss, and T. P. Das, Phys. Rev. **B19** (1979), 5525.

17. J. H. Van Vleck, J. Phys. Chem. **41** (1937), 67.

18. B. R. Judd, Phys. Rev. **127** (1962), 750.

19. G. S. Ofelt, J. Chem. Phys. **37** (1962), 511.

20. M. E. Rose, *Elementary Theory of Angular Momentum*, Wiley, New York (1957).

21. C. J. Ballhausen, *Introduction to Ligand Field Theory*, McGraw-Hill, New York (1962).

22. H. Lachwa and D. Reinen, Inorg. Chem. **28** (1989), 1044.

Distribution

Administrator
Defense Technical Information Center
Attn: DTIC-DDA (2 copies)
Cameron Station, Building 5
Alexandria, VA 22304-6145

Director
Defense Advanced Research Projects Agency
Attn: J. Friebele
1400 Wilson Blvd
Arlington, VA 22290

Director
Defense Nuclear Agency
Attn: Tech Library
Washington, DC 20305

Undersecretary of Defense Res & Engineering
Attn: Technical Library, 3C128
Washington, DC 20301

Office of the Deputy Chief of Staff for Res, Devl, & Acq
Department of the Army
Attn: DAMA-ARZ-B, I. R. Hershner
Washington, DC 20310

Commander
US Army Armament Munitions & Chemical (AMCCOM) R&D Command
Attn: SMCAR-TSS, STINFO Div
Dover, NJ 07801

Commander
Atmospheric Sciences Laboratory
Attn: Technical Library
White Sands Missile Range, NM 88002

Director
US Army Ballistics Research Laboratory
Attn: SLCBR-DD-T (STINFO)
Aberdeen Proving Ground, MD 21005

US Army Electronics Warfare Laboratory
Attn: AMSEL-DD, J. Charlton
FT Monmouth, NJ 07703

Commanding Officer
US Foreign Science & Technology Center
Attn: AIAST-BS, Basic Science Div
Federal Office Building
Charlottesville, VA 22901

Commander
US Army Materials & Mechanics Research Center
Attn SLCMT-TL, Tech Library
Watertown, MA 02172

Director
US Army Materiel Systems Analysis Activity
Attn AMXSY-MP, Library
Aberdeen Proving Ground, MD 21005

Commander
US Army Missile & Munitions Center & School
Attn: AMSMI-TB, Redstone Sci Info Center
Redstone Arsenal, AL 35809

Director
Night Vision & Electro-Optics Lab, LABCOM
Attn: Technical Library
Attn: R. Buser
Attn: A. Pinto
Attn: J. Hebersat
Attn: R. Rhode
Attn: W. Tressel
Attn: L. Merkel
FT Belvoir, VA 22060

Commander
US Army Research Office Durham
Attn: C. Bogosian
Attn: M. Ciftan
Attn: M. Stosio
Attn: R. Guenther
Attn: R. J. Lontz
Research Triangle Park, NC 27709

Commander
USA Rsch & Std Gp (Europe)
Attn Chief, Physics & Math Branch
FPO, New York 09510

Distribution

Commander
US Army Test & Evaluation Command
Attn: D. H. Sliney
Attn: Tech Library
Aberdeen Proving Ground, MD 21005

Commander
US Army Troop Support Command
Attn: STRNC-RTL, Tech Library
Natick, MA 01762

Director
Naval Research Laboratory
Attn: Code 2620, Tech Library Br
Attn: G. Quarles
Attn: G. Kintz
Attn: A. Rosenbaum
Attn: G. Risenblatt
Attn: Code 5554, F. Bartoli
Attn: Code 6540, S. R. Bowman
Attn: Code 5554, L. Esterowitz
Attn: Code: 5554, R. E. Allen
Washington, DC 20375

Commander
Naval Weapons Center
Attn: Code 3854, M. Hills
Attn: Code 3854, M. Nader
Attn: Code 3854, R. L. Atkins
Attn: Code 3854, R. Schwartz
Attn: DOCE343, Technical Information Dept
China Lake, CA 93555

Department of Commerce
National Institute of Science and Technology
Attn: Library
Washington, DC 20234

NASA Langley Research Center
Attn: N. P. Barnes
Attn: G. Armagen
Attn: C. Bair
Attn: E. Filer
Attn: F. Allario
Attn: J. Barnes
Attn: M. Buoncristiani

NASA Langley Research Center (cont'd)
Attn: N. Y. Chou
Attn: P. Cross
Hampton, VA 23665

Argonne National Laboratory
Attn: W. T. Carnall
9700 South Cass Avenue
Argonne, IL 60439

Oak Ridge National Laboratory
Attn : R. G. Haire
Oak Ridge, TN 37839

Director
Advisory Group on Electron Devices
Attn: Sectry, Working Group D
201 Varick Street
New York, NY 10013

Aerospace Corporation
Attn : M. Birnbaum
Attn: N. C. Chang
Attn : T. S. Rose
PO Box 92957
Los Angeles, CA 90009

Allied Signal Inc
Attn: R. Morris
POB 1021R
Morristown, NJ 07960

Ames Laboratory Dow
Iowa State University
Attn: K. A. Gschneidner, Jr. (2 copies)
Ames, IA 50011

Booz Allen and Hamilton
Attn: W. Drozdoski
4330 East West Highway
Bethesda, MD 20814

Draper Lab
Attn: F. Hakimi
MS 53555 Tech Sq
Cambridge, MA 02139

Distribution

Engineering Societies Library
Attn: Acquisitions Dept
345 E. 47th Street
New York, NY 10017

Fibertech, Inc.
Attn: H. R. Verdin (3 copies)
510-A Herdon Pkwy
Herdon, VA 22070

Hughes Aircraft Company
Attn: D. Sumida
3011 Malibu Canyon Rd
Malibu, CA 90265

IBM Research Division
Almaden Research Center
Attn: R. M. Macfarlane, Mail Stop K32 802(d)
650 Harry Road
San Jose, CA 95120

Director
Lawrence Radiation Laboratory
Attn: H. A. Koehler
Attn: M. J. Weber
Attn: W. Krupke
Livermore, CA 94550

LTV
Attn: M. Kock (WT-50)
PO Box 650003
Dallas, TX 75265

Martin Marietta
Attn: F. Crowne
Attn: J. Little
Attn: T. Worchesky
1450 South Rolling Road
Baltimore, MD 21227

McDonnell Douglass Electronic Systems
Company
Dept Y440, Bldg. 101, Lev. 2,Rm/PT b54
Attn: D. M. Andrauskas, MS-2066267
PO Box 516
ST Louis, MO 63166

MIT Lincoln Lab
Attn: B. Aull
PO Box 73
Lexington, MA 02173

Department of Mech, Indus, & Aerospace Eng
Attn: S. Temkin
PO Box 909
Piscataway, NJ 08854

National Oceanic & Atmospheric Adm
Environmental Research Labs
Attn Library, R-51, Tech Rpts
Boulder, CA 80302

Science Applications International Corp
Attn: T. Allik
1710 Goodridge Drive
McLean, VA 22102

Swartz Electro-Optic, Inc
Attn: G. A. Rines
45 Winthrop Street
Concord, MA 01742

W. J. Schafer Assoc
Attn: J. W. Collins
321 Billerica Road
Chelmsford, MA 01824

Union Carbide Corp
Attn: M. R. Kokta
50 South 32nd Street
Washougal, WA 98671

Arizona State University
Dept of Chemistry
Attn: L. Eyring
Tempe, AZ 85281

Bishop's University
Attn: A. Brown
Quebec, Canada

University of Southern California
Attn: M. Birnbaum
Denney Research Bldg., University Park
Los Angeles, CA 90089

Distribution

Carnegie Mellon University
Schenley Park
Attn: Physics & EE, J. O. Artman
Pittsburgh, PA 15213

Colorado State University
Physics Department
Attn: S. Kern
FT Collins, CO 80523

Concordia University
Dept of Chem. and Biochem.
Attn: G. Cormier (10 copies)
Attn: J. Capobianco (10 copies)
Attn: N. Raspa
Attn: P.-P. Proulx
1455 de Maissoneuve Blvd W
Montreal, Quebec H3G1M8, Canada

University of Connecticut
Dept of Physics
Attn: R. H. Bartram
Storrs, CT 06269

University of South Florida
Physics Dept
Attn: Sengupta
Attn: R. Chang
Tampa, FL 33620

University of Georgia
Dept of Phys. and Astron
Attn: H. Eilers
Attn: K. Hoffman
Attn: S. Jacobsen
Athens, GA 30602

City Polytechnic of Hong Kong
Attn: C. Rudowicz
Tat Chee Avenue
Kowloon, Hong Kong

Hong Kong Polytechnic
Attn: Y. Y. Yeung
Hung Hom, Kowloon
Hong Kong

Howard University
Department of Physics
Attn: Prof. V. Kushamaha
25 Bryant St., NW
Washington, DC 20059

Johns Hopkins University
Dept of Physics
Attn: B. R. Judd
Baltimore, MD 21218

Kalamazoo College
Dept of Physics
Attn: K. Rajnak
Kalamazoo, MI 49007

Massachusetts Institute of Technology
Crystal Physics Laboratory
Attn: H. P. Jenssen
Attn: A. Linz
Cambridge, MA 02139

University of Minnesota, Duluth
Department of Chemistry
Attn: L. C. Thompson
Duluth, MN 55812

Pennsylvania State University
Materials Research Laboratory
Attn: W. B. White
University Park, PA 16802

Princeton University
Department of Chemistry
Attn: D. S. McClure
Princeton, NJ 08544

San Jose State University
Department of Physics
Attn: J. B. Gruber
San Jose, CA 95192

Seton Hall University
Chemistry Department
Attn: H. Brittain
South Orange, NJ 07099

Distribution

University of Virginia
Dept of Chemistry
Attn: F. S. Richardson (2 copies)
Charlottesville, VA 22901

University of Wisconsin
Chemistry Department
Attn: J. Wright
Attn: B. Tissue
Madison, WI 53706

Departmento de Química Fundamental and
Departmento de Fisica
Attn: G. F. de Sá
Attn: W. M. de Azevedo
Attn: O. L. Malta
da UFPE, Cidade, Universitaria,
50,000, Recife, PE-Brasil

Laboratoire de Physico-Chimie
des Materiaux Luminescents
Attn: R. Moncorgé (10 copies)
Université de Lyon
URA 442 CNRS
69622 Villeurbanne, France

ENEA Thin Film Laboratory
Attn: G. Salvetti
ZIA Anguillarese, 301
00060 Roma, Italy

US Army Laboratory Command
Attn: AMSLC-DL, Dir Corp Labs

S^3 Processing Technology Organization
Attn: SLCTO, B. Weber

Installation Support Activity
Attn: SLCIS-CC-IP, Legal Office

USAISC
Attn: AMSLC-IM-VA, Admin Ser Br
Attn: AMSLC-IM-VP, Tech Pub Br (2 copies)

Harry Diamond Laboratories
Attn: Laboratory Directors
Attn: SLCHD-CS, Chief Scientist
Attn: SLCHD-NW-EP, C. S. Kenyon
Attn: SLCHD-NW-EP, J. R. Miletta
Attn: SLCHD-NW-RP, B. McLean
Attn: SLCHD-PO, Chief
Attn: SLCHD-SD-TL, Library (3 copies)
Attn: SLCHD-SD-TL, Library (Woodbridge)
Attn: SLCHD-ST-AP, T. Bahder
Attn: SLCHD-ST-AP, J. Bradshaw
Attn: SLCHD-ST-AP, J. Bruno
Attn: SLCHD-ST-AP, G. Bryant
Attn: SLCHD-ST-AP, E. Harris
Attn: SLCHD-ST-AP, R. Leavitt
Attn: SLCHD-ST-AP, J. Pham
Attn: SLCHD-ST-AP, D. Richardson
Attn: SLCHD-ST-AP, G. Simonis
Attn: SLCHD-ST-AP, M. Stead
Attn: SLCHD-ST-AP, R. Tober
Attn: SLCHD-ST-AP, M. Tobin
Attn: SLCHD-ST-AP, D. Wortman
Attn: SLCHD-ST-OP, C. Garvin
Attn: SLCHD-ST-OP, J. Goff
Attn: SLCHD-ST-R, A. A. Bencivenga
Attn: SLCHD-ST-SP, Chief
Attn: SLCHD-ST-SP, J. Nemarich
Attn: SLCHD-TA-AS, G. Turner
Attn: SLCHD-TA-ET, B. Zabludowski
Attn: SLCHD-ST-AP, C. Morrison (10 copies)